AIMS Mathematics, 8(1): 1737–1756.
DOI: 10.3934/math.2023089
Received: 11 August 2022
Revised: 05 October 2022
Accepted: 11 October 2022
Published: 24 October 2022

http://www.aimspress.com/journal/Math

Research article

Dynamical behavior of a stochastic highly pathogenic avian influenza A (HPAI) epidemic model via piecewise fractional differential technique

Maysaa Al-Qureshi[1,2], Saima Rashid[3,*], Fahd Jarad[4,5,6,*] and Mohammed Shaaf Alharthi[7]

[1] Department of Mathematics, King Saud University, P.O.Box 22452, Riyadh 11495, Saudi Arabia
[2] Department of Mathematics, Saudi Electronic University, Riyadh, Saudi Arabia
[3] Department of Mathematics, Government College university, Faislabad, pakistan
[4] Department of Mathematics, Çankaya University, Ankara, Turkey
[5] Department of Medical Research, China Medical University Hospital, China Medical University, Taichung, Taiwan
[6] Department of Mathematics, King Abdulaziz University, Jeddah, Saudi Arabia
[7] Department of Mathematics and Statistics, College of Science, Taif University, P.O.Box 11099, Taif 21944, Saudi Arabia

* **Correspondence:** Email: saimarashid@gcuf.edu.pk, fahd@cankaya.edu.tr.

Abstract: In this research, we investigate the dynamical behaviour of a HPAI epidemic system featuring a half-saturated transmission rate and significant evidence of crossover behaviours. Although simulations have proposed numerous mathematical frameworks to portray these behaviours, it is evident that their mathematical representations cannot adequately describe the crossover behaviours, particularly the change from deterministic reboots to stochastics. Furthermore, we show that the stochastic process has a threshold number $\mathbf{R}_0^s$ that can predict pathogen extermination and mean persistence. Furthermore, we show that if $\mathbf{R}_0^s > 1$, an ergodic stationary distribution corresponds to the stochastic version of the aforementioned system by constructing a sequence of appropriate Lyapunov candidates. The fractional framework is expanded to the piecewise approach, and a simulation tool for interactive representation is provided. We present several illustrated findings for the system that demonstrate the utility of the piecewise estimation technique. The acquired findings offer no uncertainty that this notion is a revolutionary viewpoint that will assist mankind in identifying nature.

Keywords: HPAI epidemic model; Atangana-Baleanu operator; piecewise numerical scheme; ergodicity and stationary distribution; extinction
Mathematics Subject Classification: 46S40, 47H10, 54H25

1. Introduction

Because we encounter a variety of hazardous contagious illnesses on a regular basis, developing appropriate mathematical simulations and combating contagious infections has proven progressively crucial in recent decades. Vaccination is an infectious agent approach for infections including seasonal flu, tetanus, pneumonia, smallpox, and others. HPAI H5N6, an avian influenza A variant, is a pathogen that transforms through H5N1, a similar form of avian influenza infection that is as dangerous as H5N6. According to [1], the highly contagious viral H5N6, which would be visible in all bird species, is expected to be the most recent extremely enteric bacteria strain to emerge in Beijing since July 2014. H5N6 influenza viruses with lower virulence had previously emerged in many parts of the world, including Europe (1984), Scandinavia (2002), and the United States (1975, 2013), but the effects on the livestock industry and environmental safety were minor. In contrast to previous incidents, the HPAI H5N6 that emerged in Beijing (2014) severely attacked and endangered birds and living beings [2].

According to research, all occurrences of H5N6 in individuals have had interaction involving live poultry exchanges. Despite the chance of this virus's transmission from chickens to individuals being considered minimal, there have been 16 incidences of H5N6 significantly entering the bloodstream and six fatalities from China [2, 3]. 11 people were found to be contaminated by the lethal infection in the 16 cases, resulting in a 69 percent incident morbidity incidence [3]. Nausea, diarrhoea, bronchitis, multi-organ dysfunction, dementia, cardiogenic distress, and blindness are some of the indications of H5N6 in people [4].

Although mathematical modelling investigations into H5N6 are infrequent, there have been a handful of analyses that estimate various subtypes of avian influenza for poultry and human activities [5, 6]. Several studies have chosen to use bilinear recurrence estimates to investigate avian influenza propagation, including bird and human populations, for accessibility [7]. Consequently, in an attempt to achieve a considerable reduction in the proportion of sick individuals, current avian influenza estimates have begun to assume saturated transmission rather than bilinear transmission [8].Recently, Liu et al. [9] and Zhang et al. [7] employed semilinear and partially prevalence rates to simulate the transmission of H7N9 independently. Lee and Lao [10] constructed many theories that incorporate bilinear occurrence and saturation transmission to examine the propagation of avian influenza. The avian-only half-saturated prevalence estimate considering the immunization approach is proposed by Lee and Lao [10] as follows:

$$\begin{cases} \dot{\mathbf{s}}(\xi) = (1-\mathbf{q})\Xi - \omega\mathbf{s} - \frac{\vartheta_{\mathfrak{b}}\mathbf{si}}{\mathbf{H}_{\mathfrak{b}}+\mathbf{i}}, \\ \dot{\mathbf{v}}(\xi) = \mathbf{q}\Xi - \omega\mathbf{v} - \frac{(1-\phi)\vartheta_{\nu}\mathbf{vi}}{\mathbf{H}_{\nu}+\mathbf{i}}, \\ \dot{\mathbf{i}}(\xi) = \frac{\vartheta_{\mathfrak{b}}\mathbf{si}}{\mathbf{H}_{\mathfrak{b}}+\mathbf{i}} - \frac{(1-\phi)\vartheta_{\nu}\mathbf{vi}}{\mathbf{H}_{\nu}+\mathbf{i}} - (\omega+\lambda)\mathbf{i}, \end{cases} \tag{1.1}$$

where $\mathbf{s}(\xi)$, $\mathbf{v}(\xi)$ and $\mathbf{v}(\xi)$ represent vulnerable, immunized, and contagious people at time step ξ, respectively. Ξ signifies a steady pace of acquisition of vulnerable people; $\mathbf{q}$ represents the immunization program's high incidence; the factor ω represents the specie's normal fatality rate; $\vartheta_{\mathfrak{b}}$ represents the spread of infection rate when vulnerable people come into contact with infectious patients; ϑ_{ν} represents the proportion of immunised birds that acquire avian influenza; λ represents infection fatality; and ϕ represents vaccination effectiveness; the half-saturation parameter for avian pathogen sensitive birds is implied by $\mathbf{H}_{\mathfrak{b}}$ and the half-saturation parameter for avian pathogen sensitive birds is implied by $\mathbf{H}_{\nu}$signifies the half-saturation value for avian variant inoculated birds.

Several key conclusions in classical calculus were published in the eighteenth century by notable researchers including Liouville, Riemann, Euler, Fourier, and many others [11–14]. Non-locality is a major motivator for attention in fractional calculus implementations [15–17]. There are numerous fascinating occurrences that exhibit what are known as memory influences, which means that their existence is dependent not just on time and location but also on their original configuration. Recently, fractional differential equations have been used in thermodynamics, thermoplastic flowability, regular variation in heat transfer, biostatistics, blood circulation anomalies, wind resistance, electromagnetics, deformability, capacitance concept, electrical connections, molecular biology, cognitive science, and appropriate scientific results. In previous studies, various forms of nonlocal fractional derivatives have subsequently been proposed to tackle the elimination of derivative operators having power-law. Caputo-Fabrizio [18], for example, presented a fresh fractional derivative predicated on the exponential kernel. Meanwhile, this operator is experiencing significant difficulties with the kernel's placement. Atangana and Baleanu developed a unique improved formulation of a fractional derivative using the Mittag-Leffler function as a non-local and non-singular kernel in [19] to alleviate CaputoFabrizios turmoil. The Atangana-Baleanu-Caputo (ABC) fractional derivative accurately describes the memory [20–22]. The ABC operator's most noteworthy uses can be discovered in [23–25]. This generalized Mittag-Leffler kernel can, however, describe crossover from conventional to sub-diffusion as well as crossover from stochastic process to power-law. Moreover, this kernel cannot detect crossover from deterministic to stochastic settings or from stochastic to deterministic environments, which is a significant drawback of such operators in these cases [26, 27]. Atangana and Seda [28] subsequently proposed the ideas of piecewise differential/integral formulations. Furthermore, they expanded their novel notion of simulation by proposing piecewise modelling. This revolutionary notion may represent the destiny of modelling, as we propose in this work a creative pathway to simulate epidemiological concerns involving crossover tendencies. Furthermore, it has been discovered that fractional DEs can be used to simulate global occurrences relatively precisely [29–32]. The global problem of infection propagation drew the interest of scholars from numerous domains, resulting in the establishment of a variety of ideas to assess and predict the progress of the outbreak; for more information, see [33, 34].

The goal of this research is to examine the mechanisms of NPAI infection by employing the revolutionary notion of the piecewise fractional framework in the context of the Atangana-Baleanu derivative. We used NPAI infection with half saturation data to determine the terms and demonstrate that the current structure employing a piecewise technique yields effective adaptation to the results proposed by [10]. The modeling computations are illustrated graphically to demonstrate the theories developed. Therefore, when environmental perturbations are considered, determining the threshold of randomized infectious systems becomes problematic. Several stochastic systems no longer have non-negative steady states. As a result, the stationary distribution of stochastic processes has garnered a lot of consideration. We focus on analyzing the stochastic NPAI model's having half-saturated incidences and attempting to provide a criterion for infection extermination and permanence, as well as studying the stochastic model's stationary distribution.

2. Model depiction

Recently, researchers discovered that white noise can disrupt the transmission of contagious diseases, internal migration, and the formulation of preventive mechanisms. The appropriate stochastic frameworks have been investigated by researchers [35]. In 2021, authors [36] presented a novel notion for analyzing and predicting the transmission of COVID-19 throughout Africa and Europe using stochastic and deterministic methods. Rashid et al. [37, 38] contemplated the stochastic fractal-fractional tuberculosis model via a non-singular kernel with random densities and hepatitis B virus infection model, respectively. The novel dynamics of a stochastic fractal-fractional immune effector response to viral infection via latently infectious tissues are investigated by Rashid et al. [39]. Adopting the propensity of Zhou et al. [40], the stochastic random densities are assumed to be independent and directly proportional to $\mathbf{s}(\xi)$, $\mathbf{v}(\xi)$ and $\mathbf{i}(\xi)$. The DEs can then be used to characterize the stochastic form of the scheme (1.1) is presented in the schematic diagram Figure 1.

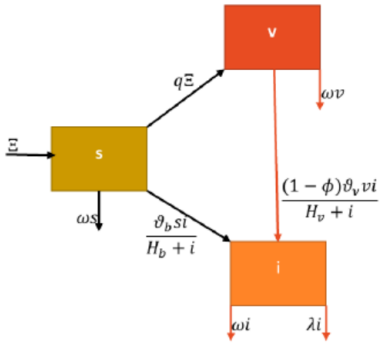

Figure 1. Flow diagram for HPIA epidemic model.

2.1. Piecewise NPAI model

This part explores the framework (1.1) in Atangana-Baleanu piecewise fractional differential equations. To accomplish this, we formulate the model (1.1) in piecewise DEs, which are provided by:

$$\begin{cases} \dot{\mathbf{s}}(\xi) = (1-\mathbf{q})\Xi - \omega\mathbf{s} - \frac{\vartheta_b \mathbf{si}}{\mathbf{H_b}+\mathbf{i}}, \\ \dot{\mathbf{v}}(\xi) = \mathbf{q}\Xi - \omega\mathbf{v} - \frac{(1-\phi)\vartheta_v \mathbf{vi}}{\mathbf{H_v}+\mathbf{i}}, \\ \dot{\mathbf{i}}(\xi) = \frac{\vartheta_b \mathbf{si}}{\mathbf{H_b}+\mathbf{i}} - \frac{(1-\phi)\vartheta_v \mathbf{vi}}{\mathbf{H_v}+\mathbf{i}} - (\omega+\lambda)\mathbf{i}, \end{cases} \tag{2.1}$$

$$\begin{cases} {}^{ABC}_{0}\mathbf{D}^{\alpha}_{\xi}\mathbf{s}(\xi) = (1-\mathbf{q})\Xi - \omega\mathbf{s} - \frac{\vartheta_b \mathbf{si}}{\mathbf{H_b}+\mathbf{i}}, \\ {}^{ABC}_{0}\mathbf{D}^{\alpha}_{\xi}\mathbf{v}(\xi) = \mathbf{q}\Xi - \omega\mathbf{v} - \frac{(1-\phi)\vartheta_v \mathbf{vi}}{\mathbf{H_v}+\mathbf{i}}, \\ {}^{ABC}_{0}\mathbf{D}^{\alpha}_{\xi}\mathbf{i}(\xi) = \frac{\vartheta_b \mathbf{si}}{\mathbf{H_b}+\mathbf{i}} - \frac{(1-\phi)\vartheta_v \mathbf{vi}}{\mathbf{H_v}+\mathbf{i}} - (\omega+\lambda)\mathbf{i}, \end{cases} \tag{2.2}$$

$$\begin{cases} \mathrm{d}\mathbf{s}(\xi) = ((1-\mathbf{q})\Xi - \omega\mathbf{s} - \frac{\vartheta_b \mathbf{si}}{\mathbf{H_b}+\mathbf{i}})\mathrm{d}\xi + \wp_1\mathbf{s}(\xi)\mathrm{d}\mathcal{B}_1(\xi), \\ \mathrm{d}\mathbf{v}(\xi) = (\mathbf{q}\Xi - \omega\mathbf{v} - \frac{(1-\phi)\vartheta_v \mathbf{vi}}{\mathbf{H_v}+\mathbf{i}})\mathrm{d}\xi + \wp_2\mathbf{v}(\xi)\mathrm{d}\mathcal{B}_2(\xi), \\ \mathrm{d}\mathbf{i}(\xi) = (\frac{\vartheta_b \mathbf{si}}{\mathbf{H_b}+\mathbf{i}} - \frac{(1-\phi)\vartheta_v \mathbf{vi}}{\mathbf{H_v}+\mathbf{i}} - (\omega+\lambda)\mathbf{i})\mathrm{d}\xi + \wp_3\mathbf{i}(\xi)\mathrm{d}\mathcal{B}_3(\xi), \end{cases} \tag{2.3}$$

In the preceding frameworks (2.1)–(2.3), we allocate time periods $\xi \in [0, \mathbf{T}_1]$, $\xi \in [\mathbf{T}_1, \mathbf{T}_2]$ and $[\mathbf{T}_2, \mathbf{T}]$ accordingly. For $\alpha \geq 0$ and $\wp_\iota$, $\iota = 1, 2, 3$ specifies the non-negative white noises, whereas the formulation of the Atangana-Baleanu derivative and the corresponding piecewise DEs findings are represented below:

$$ {}_0^{ABC}\mathbf{D}_\xi^\alpha \mathcal{F}_1(\xi) = \frac{ABC(\alpha)}{1-\alpha} \int_0^\xi \mathcal{F}_1'(\theta) E_\alpha\Big(-\frac{\alpha}{1-\alpha}(\xi-\theta)^\alpha \Big) d\theta, \tag{2.4} $$

where $ABC(\alpha) = 1 - \alpha + \frac{\alpha}{\Gamma(\alpha)}$ signifies the normalization function.

3. Dynamical aspects of stochastic NPAI epidemic model

In this paper, suppose a complete probability space $(\Theta, \mathcal{F}, \{\mathcal{F}_\xi\}_{\xi\geq 0}, \mathbf{P})$ fulfilling the given assumptions (That are., it is nondecreasing and right continuous whilst $\mathcal{F}_0$ have all empty sets $\mathbf{P}$), indicating $\mathbf{R}_+ = [0, \infty)$, $\mathbf{R}_+^d = \{\mathbf{x} = (\mathbf{x}_1, ..., \mathbf{x}_d) \mid \mathbf{x}_i > 0,\ i \in [1, d]\}$. Also, there is an integral mapping $\mathcal{F}_1(\xi)$ defined on $[0, \infty)$. introducing $\mathcal{F}_1^u = \sup\{\mathcal{F}_1(\xi) \mid \xi \geq 0\}$, $\mathcal{F}_1^l = \inf\{\mathcal{F}_1(\xi) \mid \xi \geq 0\}$.

Next, we will examine at the d-dimensional stochastic DE

$$ d\mathbf{Y}(\xi) = \mathcal{F}_1(\mathbf{Y}(\xi), \xi)\mathrm{d}\xi + \mathcal{G}(\mathbf{Y}(\xi), \xi) dB(\xi), \quad t \geq t_0, $$

subject to intial condition $\mathbf{Y}(0) = X_0 \in \mathbf{R}^d$, $B(\xi)$ denotes a d-dimensional standard Brownian motion presented on the complete probability space $(\Theta, \mathcal{F}, \{\mathcal{F}_\xi\}_{\xi\geq 0}, \mathbf{P})$. Suppose $\mathbb{C}^{2,1}(\mathbf{R}^d \times [t_0, \infty]; \mathbf{R}_+)$ the collection of all positive $\mathcal{H}(\mathbf{x}, \xi)$ on $\mathbf{R}^d \times [t_0, \infty]$ such that continuous twice differentiable in $\mathbf{Y}$ and once in ξ. The differential operator $\mathbb{L}$ is proposed by [41]:

$$ \mathbb{L} = \frac{\partial}{\partial \xi} + \sum_{\iota=1}^{d_1} f_\iota(\mathbf{Y}, \xi) \frac{\partial}{\partial X_\iota} + \frac{1}{2} \sum_{\iota,\kappa=1}^{d_1} [\mathcal{G}^{\mathbf{T}}(\mathbf{Y}, \xi)\mathcal{G}(\mathbf{Y}, \xi)]_{\iota\kappa} \frac{\partial^2}{\partial X_\iota \partial X_\kappa}. $$

Now $\mathbb{L}$ imposed on a mapping $\mathcal{H} \in \mathbb{C}^{2,1}(\mathbf{R}^d \times [t_0, \infty]; \mathbf{R}_+)$, we have

$$ \mathbb{L}\mathcal{H}(\mathbf{Y}, \xi) = \mathcal{H}_\xi(\mathbf{Y}, \xi) + \mathcal{H}_{\mathbf{x}}(\mathbf{Y}, \xi)\mathcal{F}_1(\mathbf{Y}, \xi) + \frac{1}{2} trac[\mathcal{G}^{\mathbf{T}}(\mathbf{Y}, \xi)\mathcal{H}_{\mathbf{xx}}\mathcal{G}(\mathbf{Y}, \xi)], $$

where $\mathcal{H}_\xi = \frac{\partial \mathcal{H}}{\partial \xi}, \mathcal{H}_{\mathbf{x}} = (\frac{\partial \mathcal{H}}{\partial \mathbf{x}_1}, ..., \frac{\partial \mathcal{H}}{\partial \mathbf{x}_d})$, $\mathcal{H}_{\mathbf{xx}} = (\frac{\partial^2 \mathcal{H}}{\partial \mathbf{x}_\iota \partial \mathbf{x}_\kappa})_{d_1 \times d_1}$. By the Itô's technique, if $\mathbf{Y}(\xi) \in \mathbf{R}^{d_1}$, then

$$ \mathrm{d}\mathcal{H}(\mathbf{Y}(\xi), \xi) = \mathbb{L}\mathcal{H}(\mathbf{Y}(\xi), \xi)\mathrm{d}\xi + \mathcal{H}_{\mathbf{x}}(\mathbf{Y}(\xi), \xi)\mathcal{G}(\mathbf{Y}(\xi), \xi)\mathrm{d}B(\xi). $$

3.1. Existence-uniqueness of the global non-negative solution

Theorem 3.1. *For every $\xi \geq 0$ a.s., system* (2.3) *has a unique global solution* $(\mathbf{s}(\xi), \mathbf{v}(\xi), \mathbf{i}(\xi)) \in \mathbb{R}_+^3$ *for any given initial value* $(\mathbf{s}(0), \mathbf{v}(0), \mathbf{i}(0)) \in \mathbf{R}_+^3$.

Proof. Our argument is predicated on the research of Mao et al. [42]. Because the parameters of scheme (2.3) are Lipschitz continuous locally. As a result, there is a unique local solution $(\mathbf{s}, \mathbf{v}, \mathbf{i})$ on $\xi \in (0, \varphi_0)$ for every ICs $(\mathbf{s}(0), \mathbf{v}(0), \mathbf{i}(0)) \in \mathbf{R}_+^3$, where φ_0 is the moment of the explosive. We simply require to demonstrate $\varphi_0 = \infty$ (a.s). to show the local solution is global. Allow $\mathbb{k}_0$ to be large

enough for each factor of $(\mathbf{s}(0), \mathbf{v}(0), \mathbf{i}(0))$ inside this interval $[1/\Bbbk_0, \Bbbk_0]$ for every integer $\Bbbk \geq \Bbbk_0$, now introducing the stopping time,

$$\varphi_{\Bbbk} = \inf\{\xi \in [0, \varphi_0] \mid \min\{\mathbf{s}(\xi), \mathbf{v}(\xi), \mathbf{i}(\xi)\} \leq \frac{1}{\Bbbk} \; or \; \max\{\mathbf{s}(\xi), \mathbf{v}(\xi), \mathbf{i}(\xi)\} \geq \Bbbk\}.$$

Setting $\inf \emptyset = \infty$. Note that when $\Bbbk \mapsto \infty$ then $\varphi_{\Bbbk}$ is nondecreasing. Taking $\varphi_\infty = \lim_{\Bbbk \mapsto \infty} \varphi_{\Bbbk}$, therefore $\varphi_\infty \leq \varphi_0$ $(a.s)$. We intend to prove $\varphi_\infty = \infty$ $(a.s)$ then $\varphi_0 = \infty$ $(a.s)$, which implies that $(\mathbf{s}, \mathbf{v}, \mathbf{i}) \in \mathbf{R}^3_+, \; \forall \xi \geq 0$. Also, if φ_∞ $(a.s)$, then there are two constants $\mathbf{T} \geq 0$ and $\epsilon \in (0, 1)$ such that $\mathbf{P}\{\varphi_\infty \leq \mathbf{T}\} \geq \epsilon$. Therefore, there is an integer $\Bbbk_1 \geq \Bbbk_0$ such that

$$\mathbf{P}\{\varphi_{\Bbbk} \leq \mathbf{T}\} \geq \epsilon, \; \forall \Bbbk \geq \Bbbk_1. \tag{3.1}$$

Defining a functional $\hat{\mathcal{H}} : \mathbf{R}^3_+ \mapsto \mathbf{R}_+$, *that is*,

$$\hat{\mathcal{H}}(\mathbf{s}, \mathbf{v}, \mathbf{i}) = (\mathbf{s} + \mathbf{v} + \mathbf{i}) - 3 - \ln(\mathbf{s} + \mathbf{v} + \mathbf{i}).$$

In accordance with the criteria of $(u_1 - \ln u_1 - 1) \geq 0$ as $u_1 \geq 0$, we find $\hat{\mathcal{H}}(\mathbf{s}, \mathbf{v}, \mathbf{i})$ is a positive $\mathbb{C}^2$ mapping.

Implementing Itô's technique, we have

$$\hat{\mathcal{H}}(\mathbf{s}, \mathbf{v}, \mathbf{i}) = \mathbb{L}\hat{\mathcal{H}}(\mathbf{s}, \mathbf{v}, \mathbf{i})\mathrm{d}\xi + \wp_1(\mathbf{s} - 1)\mathrm{d}\mathcal{B}_1(\xi) + \wp_2(\mathbf{v} - 1)\mathrm{d}\mathcal{B}_2(\xi) + \wp_3(\mathbf{i} - 1)\mathrm{d}\mathcal{B}_3(\xi),$$

where

$$\begin{aligned}
\mathbb{L}\hat{\mathcal{H}}(\mathbf{s}, \mathbf{v}, \mathbf{i}) \quad &= \Big(\frac{\mathbf{s} - 1}{\mathbf{s}}\Big)\Big\{(1 - \mathbf{q})\Xi - \omega\mathbf{s} - \frac{\vartheta_{\mathfrak{b}}\mathbf{s}\mathbf{i}}{\mathbf{H}_{\mathfrak{b}} + \mathbf{i}}\Big\} + \frac{1}{2}\wp_1^2 \\
&\quad + \Big(\frac{\mathbf{v} - 1}{\mathbf{v}}\Big)\Big\{\mathbf{q}\Xi - \omega\mathbf{v} - \frac{(1 - \phi)\vartheta_\nu\mathbf{v}\mathbf{i}}{\mathbf{H}_\nu + \mathbf{i}}\Big\} + \frac{1}{2}\wp_2^2 \\
&\quad + \Big(\frac{\mathbf{i} - 1}{\mathbf{i}}\Big)\Big\{\frac{\vartheta_{\mathfrak{b}}\mathbf{s}\mathbf{i}}{\mathbf{H}_\nu + \mathbf{i}} + \frac{(1 - \phi)\vartheta_\nu\mathbf{v}\mathbf{i}}{\mathbf{H}_\nu + 1} - (\omega + \lambda)\mathbf{i}\Big\} + \frac{1}{2}\wp_3^2 \\
&\leq \Xi + \lambda + \vartheta_{\mathfrak{b}} + (1 - \phi)\vartheta_\nu + 3\omega + \frac{1}{2}(\wp_1^2 + \wp_2^2 + \wp_3^2) : \Phi_1.
\end{aligned}$$

Therefore, we find

$$\mathbb{L}\hat{\mathcal{H}}(\mathbf{s}, \mathbf{v}, \mathbf{i}) \leq \Phi_1\mathrm{d}\xi + \Big\{\wp_1(\mathbf{s} - 1)\mathrm{d}\mathcal{B}_1(\xi) + \wp_2(\mathbf{v} - 1)\mathrm{d}\mathcal{B}_2(\xi) + \wp_3(\mathbf{i} - 1)\mathrm{d}\mathcal{B}_3(\xi)\Big\}.$$

Applying integration over 0 to $\varphi_{\Bbbk\wedge\mathbf{T}}$ and considering expectation, we have

$$\begin{aligned}
\mathbb{E}\hat{\mathcal{H}}(\mathbf{s}(\varphi_{\Bbbk\wedge\mathbf{T}}), \mathbf{v}(\varphi_{\Bbbk\wedge\mathbf{T}}), \mathbf{i}(\varphi_{\Bbbk\wedge\mathbf{T}})) \quad &\leq \Phi_1\mathbb{E}(\varphi_{\Bbbk\wedge\mathbf{T}}) + \hat{\mathcal{H}}(\mathbf{s}(0), \mathbf{v}(0), \mathbf{i}(0)) \\
&\leq \Phi_1\mathbf{T} + \hat{\mathcal{H}}(\mathbf{s}(0), \mathbf{v}(0), \mathbf{i}(0)).
\end{aligned}$$

For $\Bbbk \geq \Bbbk_1$, suppose $\Theta_{\Bbbk} = \{\varphi_{\Bbbk} \leq \mathbf{T}\}$, from (3.1), then $\mathbf{P}(\Theta_{\Bbbk}) \geq \epsilon$. Obviously, for each $\varpi \in \Theta_{\Bbbk}$, there is one or more of $\mathbf{s}(\varphi_{\Bbbk}, \varpi), \mathbf{v}(\varphi_{\Bbbk}, \varpi), \mathbf{i}(\varphi_{\Bbbk}, \varpi)$ equals either $1/\Bbbk$ or $\Bbbk$, therefore $\tilde{\mathcal{H}}(\mathbf{s}(\varphi_{\Bbbk}, \varpi), \mathbf{v}(\varphi_{\Bbbk}, \varpi), \mathbf{i}(\varphi_{\Bbbk}, \varpi))$ is not less than either $\Bbbk - 1 \ln \Bbbk$ or $1/\Bbbk - 1 + \ln \Bbbk$, then

$$\Phi_1\mathbf{T} + \hat{\mathcal{H}}(\mathbf{s}(0), \mathbf{v}(0), \mathbf{i}(0))$$

$$\geq \mathbb{E}[\mathcal{I}_{\Theta_{\Bbbk}}(\varpi)\hat{\mathcal{H}}(\mathbf{s}(\varphi_{\Bbbk},\varpi),\mathbf{v}(\varphi_{\Bbbk},\varpi),\mathbf{i}(\varphi_{\Bbbk},\varpi))]$$
$$\geq \epsilon(\Bbbk - 1 - \ln\Bbbk) \wedge \Big(1/\Bbbk - 1 + \ln\Bbbk\Big),$$

where $\mathcal{I}_{\Theta_{\Bbbk}}(.)$ represents the indicating mapping of $\Theta_{\Bbbk}$. Thus, applying limit $\Bbbk \mapsto \infty$ yields contradiction

$$\infty = \Phi_1\mathbf{T} + \hat{\mathcal{H}}(\mathbf{s}(0),\mathbf{v}(0),\mathbf{i}(0)) < \infty.$$

Thus, we find $\varphi_\infty = \infty,\ (a.s)$. This completes the proof.

3.2. Extinction of the epidemic

One of the primary challenges in epidemiology is how to govern epidemic patterns so that the infection becomes endemic and persists throughout time. In this part, we attempt to determine the threshold quantity for pathogen extermination and permanence.

Let us define

$$\mathbf{R}_0^s = \frac{2\Xi}{2(\omega+\lambda)+\wp_3^2}\Big(\frac{(1-\mathbf{q})\vartheta_{\mathfrak{b}}\mathbf{H}_\nu + (1-\phi)\mathbf{q}\vartheta_\nu\mathbf{H}_{\mathfrak{b}}}{\omega\mathbf{H}_{\mathfrak{b}}\mathbf{H}_\nu}\Big).$$

Following the work of [24], We obtain the accompanying lemma.

Lemma 3.1. *For initial settings* $(\mathbf{s}(0),\mathbf{v}(0),\mathbf{i}(0)) \in \mathbf{R}_+^3$, *then the solution of the model* $(\mathbf{s},\mathbf{v},\mathbf{i})$ *satisfies*

$$\lim_{\xi\mapsto\infty}\frac{\ln\mathbf{s}(\xi)}{\xi} \leq 0,\quad \lim_{\xi\mapsto\infty}\frac{\ln\mathbf{v}(\xi)}{\xi} \leq 0,\quad \lim_{\xi\mapsto\infty}\frac{\ln\mathbf{i}(\xi)}{\xi} \leq 0,\ (a.s). \tag{3.2}$$

That is $\lim_{\xi\mapsto\infty}\frac{\mathbf{s}(\xi)+\mathbf{v}(\xi)+\mathbf{i}(\xi)}{\xi} = 0,\ (a.s)$. *Also, if* $\omega > \frac{1}{2}(\wp_1^2 \vee \wp_2^2 \vee \wp_3^2)$, *we find*

$$\lim_{\xi\mapsto\infty}\frac{1}{\xi}\int_0^\xi \mathbf{s}(\xi)\mathrm{d}\mathcal{B}_1(\xi) = 0,\quad \lim_{\xi\mapsto\infty}\frac{1}{\xi}\int_0^\xi \mathbf{v}(\xi)\mathrm{d}\mathcal{B}_1(\xi) = 0,\quad \lim_{\xi\mapsto\infty}\frac{1}{\xi}\int_0^\xi \mathbf{i}(\xi)\mathrm{d}\mathcal{B}_1(\xi) = 0.$$

Theorem 3.2. *Assume that there is a non-negative solution of the model* (2.3) $(\mathbf{s}(\xi),\mathbf{v}(\xi),\mathbf{i}(\xi))$ *having the initial settings* $(\mathbf{s}(0),\mathbf{v}(0),\mathbf{i}(0))$, *we find*

(i) *If* $\mathbf{R}_0^s < 1$, *then* $\limsup_{\xi\mapsto\infty}\frac{\ln\mathbf{i}(\xi)}{\xi} \leq (\omega+\lambda+\frac{\wp_3^2}{2})(\mathbf{R}_0^s - 1) < 0\ (a.s)$. *This suggests that the infection will be extinguished in the long run.*

(ii) *If* $\mathbf{R}_0^s > 1$, *then* $\liminf_{\xi\mapsto\infty}\frac{1}{\xi}\int_0^\xi \mathbf{i}(\varsigma)d\varsigma \geq \frac{(\omega+\lambda+\frac{\wp_3^2}{2})(\mathbf{R}_0^s-1)}{\Phi_2} > 0\ (a.s)$, *where*

$$\Phi_2 = \frac{\omega+\lambda}{\omega}\Big(\frac{(\omega+\vartheta_{\mathfrak{b}})\mathbf{H}_\nu + \omega(\omega+(1-\phi)\vartheta_\nu)\mathbf{H}_{\mathfrak{b}}}{\mathbf{H}_{\mathfrak{b}}\mathbf{H}_\nu}\Big).$$

This means that the sickness will be present for a long time.

Proof. Utilizing Itô's technique to $\ln\mathbf{i}(\xi)$, we find

$$d\ln\mathbf{i}(\xi) = \Big(\frac{\vartheta_{\mathfrak{b}}\mathbf{s}}{\mathbf{H}_{\mathfrak{b}}+\mathbf{i}} + \frac{(1-\phi)\vartheta_\nu\mathbf{v}}{\mathbf{H}_\nu+\mathbf{i}} - (\omega+\lambda+\frac{\wp_3^2}{2})\Big)\mathrm{d}\xi + \wp_3\mathrm{d}\mathcal{B}_3(\xi).$$

Applying integration technique from 0 to ξ, we have

$$\ln \mathbf{i}(\xi) - \ln \mathbf{i}(0) = \int_0^{\xi} \Big(\frac{\vartheta_{\mathfrak{b}\mathbf{s}}}{\mathbf{H}_{\mathfrak{b}} + \mathbf{i}} + \frac{(1-\phi)\vartheta_{\nu}\mathbf{v}}{\mathbf{H}_{\nu} + \mathbf{i}} - (\omega + \lambda + \frac{\wp_3^2}{2}) \Big) d\varsigma + \wp_3 \int_0^{\xi} \mathrm{d}\mathcal{B}_3(\varsigma).$$

In view of the strong law of large numbers [43], we have

$$\lim_{\xi \mapsto \infty} \frac{1}{\xi} \int_0^{\xi} \mathrm{d}\mathcal{B}_3(\varsigma) = 0. \ (a.s).$$

Considering the superior limit and applying the stochastic comparison concept with disease-free equilibrium $\mathcal{E}_0 = \Big(\frac{(1-p-1)\Xi}{\omega}, \frac{\mathbf{q}\Xi}{\omega}, 0 \Big)$, we get

$$\begin{aligned} \limsup_{\xi \mapsto \infty} \frac{\ln \mathbf{i}(\xi)}{\xi} &= \limsup_{\xi \mapsto \infty} \frac{1}{\xi} \int_0^{\xi} \Big(\frac{\vartheta_{\mathfrak{b}\mathbf{s}}}{\mathbf{H}_{\mathfrak{b}} + \mathbf{i}} + \frac{(1-\phi)\vartheta_{\nu}\mathbf{v}}{\mathbf{H}_{\nu} + \mathbf{i}} \Big) d\varsigma - ((\omega + \lambda + \frac{\wp_3^2}{2})) \\ &\leq \Big(\frac{(1-\mathbf{q})\vartheta_{\mathfrak{b}}\mathbf{H}_{\nu} + (1-\phi)\mathbf{q}\vartheta_{\nu}\mathbf{H}_{\mathfrak{b}}}{\omega \mathbf{H}_{\mathfrak{b}}\mathbf{H}_{\nu}} \Big) - (\omega + \lambda + \frac{\wp_3^2}{2}) \\ &= (\omega + \lambda + \frac{\wp_3^2}{2})(\mathbf{R}_0^s - 1) < 0 \ (a.s). \end{aligned}$$

As a result, it implies that $\lim_{\xi \mapsto \infty} \mathbf{i}(\xi) = 0, \ (a.s)$. which shows that the infection will be eliminated in the long run.

(ii) Define a $\mathbb{C}^2$-mapping $\mathcal{H}_1$

$$\mathcal{H}_1(\mathbf{s}, \mathbf{v}, \mathbf{i}) = -\Big(\frac{\mathbf{H}_{\mathfrak{b}} + \mathbf{H}_{\nu}}{\mathbf{H}_{\mathfrak{b}}\mathbf{H}_{\nu}} \mathbf{i} - \frac{\vartheta_{\mathfrak{b}}}{\omega} \frac{\mathbf{s} + \mathbf{i}}{\mathbf{H}_{\mathfrak{b}}} - \ln \mathbf{i} - \frac{(1-\phi)\vartheta_{\nu}}{\omega} \frac{\mathbf{v} + \mathbf{i}}{\mathbf{H}_{\nu}} \Big).$$

Implementing Itô's technique, we have

$$\begin{aligned} \mathbb{L}\mathcal{H}_1 &= (\omega + \lambda + \frac{\wp_3^2}{2}) - \frac{\vartheta_{\mathfrak{b}\mathbf{s}}}{\mathbf{H}_{\mathfrak{b}} + \mathbf{i}} - \frac{(1-\phi)\vartheta_{\nu}\mathbf{v}}{\mathbf{H}_{\nu} + \mathbf{i}} - \Big(\frac{\mathbf{H}_{\mathfrak{b}}\mathbf{H}_{\nu}}{\mathbf{H}_{\mathfrak{b}} + \mathbf{H}_{\nu}} \Big) \Big(\frac{\vartheta_{\mathfrak{b}\mathbf{s}}}{\mathbf{H}_{\mathfrak{b}} + \mathbf{i}} + \frac{(1-\phi)\vartheta_{\nu}\mathbf{v}}{\mathbf{H}_{\nu} + \mathbf{i}} - (\omega + \lambda)\mathbf{i} \Big) \\ &\quad - \frac{\vartheta_{\mathfrak{b}}}{\omega \mathbf{H}_{\mathfrak{b}}} \Big((1-\mathbf{q})\Xi - \omega \mathbf{s} + \frac{(1-\phi)\vartheta_{\nu}\mathbf{v}\mathbf{i}}{\mathbf{H}_{\nu} + \mathbf{i}} - (\omega + \lambda)\mathbf{i} \Big) \\ &\quad - \frac{(1-\phi)\vartheta_{\nu}}{\omega \mathbf{H}_{\nu}} \Big(\mathbf{q}\Xi - \omega \mathbf{v} + \frac{\vartheta_{\mathfrak{b}}\mathbf{s}\mathbf{i}}{\mathbf{H}_{\mathfrak{b}} + \mathbf{i}} - (\omega + \lambda)\mathbf{i} \Big) \\ &\leq (\omega + \lambda + \frac{\wp_3^2}{2}) - \frac{\vartheta_{\mathfrak{b}\mathbf{s}}}{\mathbf{H}_{\mathfrak{b}}} - \frac{(1-\phi)\vartheta_{\nu}\mathbf{v}}{\mathbf{H}_{\nu}} - \frac{\vartheta_{\mathfrak{b}}}{\mathbf{H}_{\mathfrak{b}}} \Big(\frac{(1-\mathbf{q})\Xi}{\omega} - \mathbf{s} \Big) - \frac{(1-\phi)\vartheta_{\nu}}{\mathbf{H}_{\nu}} \Big(\frac{\mathbf{q}\Xi}{\omega} - \mathbf{v} \Big) \\ &\quad + \frac{\omega + \lambda}{\omega} \Big(\frac{\omega + \vartheta_{\mathfrak{b}}}{\mathbf{H}_{\mathfrak{b}}} + \frac{\omega + (1-\phi)\vartheta_{\nu}}{\mathbf{H}_{\nu}} \Big) \mathbf{i} \\ &= (\omega + \lambda + \frac{\wp_3^2}{2}) - \frac{(1-\mathbf{q})\Xi\vartheta_{\mathfrak{b}}}{\omega \mathbf{H}_{\mathfrak{b}}} - \frac{(1-\phi)\mathbf{q}\Xi\vartheta_{\nu}}{\omega \mathbf{H}_{\nu}} + \Phi_2 \mathbf{i}. \end{aligned}$$

Then

$$\mathbb{L}\mathcal{H}_1 \leq -(\omega + \lambda + \frac{\wp_3^2}{2})(\mathbf{R}_0^s - 1) + \Phi_2 \mathbf{i}.$$

Assume that

$$\Phi_3 = \frac{\omega + \vartheta_{\mathfrak{b}}}{\omega \mathbf{H}_{\mathfrak{b}}} + \frac{\omega + (1-\phi)\vartheta_{\nu}}{\omega \mathbf{H}_{\nu}}.$$

Eventually, we have

$$\mathrm{d}\mathcal{H}_1(\mathbf{s}, \mathbf{v}, \mathbf{i}) = \mathbb{L}\mathcal{H}_1 \mathrm{d}\xi - \wp_3 \mathrm{d}\mathcal{B}_3(\xi) - \frac{\vartheta_b}{\omega \mathbf{H}_{\mathfrak{b}}} \wp_1 \mathrm{d}\mathcal{B}_1(\xi) - \frac{(1-\phi)\vartheta_{\nu}}{\omega \mathbf{H}_{\nu}} \wp_2 \mathbf{v} \mathrm{d}\mathcal{B}_2(\xi) - \Phi_2 \wp_3 \mathrm{d}\mathcal{B}_3(\xi).$$

Integrating above equation with respect to ξ, we have

$$\begin{aligned}
&\frac{\mathcal{H}_1(\mathbf{s}(\xi), \mathbf{v}(\xi), \mathbf{i}(\xi)) - \mathcal{H}_1(\mathbf{s}(0), \mathbf{v}(0), \mathbf{i}(0))}{\xi} \\
&\leq -(\omega + \lambda + \frac{\wp_3^2}{2})(\mathbf{R}_0^s - 1) + \frac{\Phi_2}{\xi} \int_0^{\xi} \mathbf{i}(\varsigma) d\varsigma - \frac{\mathcal{Q}(\xi)}{\xi} - \frac{\vartheta_{\mathfrak{b}}}{\omega \mathbf{H}_{\mathfrak{b}}} \frac{1}{\xi} \int_0^{\xi} \wp_1 \mathbf{s} \mathrm{d}\mathcal{B}_1(\varsigma) \\
&\quad - \frac{(1-\phi)\vartheta_{\nu}}{\omega \mathbf{H}_{\nu}} \frac{1}{\xi} \int_0^{\xi} \wp_2 \mathbf{v} \mathrm{d}\mathcal{B}_2(\varsigma) - \frac{\mathcal{K}_{\ni}}{\xi} \int_0^{\xi} \wp_3 \mathbf{i} \mathrm{d}\mathcal{B}_3(\varsigma),
\end{aligned}$$

where $\mathcal{Q}(\xi) = \int_0^{\xi} \wp_3 \mathrm{d}\mathcal{B}_3(\varsigma)$ is a martingale. In view of the strong principal of large numbers for martingales, we have

$$\lim_{\xi \mapsto \infty} \frac{\mathcal{Q}_1(\xi)}{\xi} = 0. \ (a.s). \tag{3.3}$$

Utilizing (3.3) and Lemma 3.1, we find

$$\begin{aligned}
&\liminf_{\xi \mapsto \infty} \Phi_2 \frac{1}{\xi} \int_0^{\xi} \mathbf{i}(\varsigma) d\varsigma \geq (\omega + \lambda + \frac{\wp_3^2}{2})(\mathbf{R}_0^s - 1) + \liminf_{\xi \mapsto \infty} \left(\frac{\mathcal{H}_1(\mathbf{s}(\xi), \mathbf{v}(\xi), \mathbf{i}(\xi)) - \mathcal{H}_1(\mathbf{s}(0), \mathbf{v}(0), \mathbf{i}(0))}{\xi} \right) \\
&\geq (\omega + \lambda + \frac{\wp_3^2}{2})(\mathbf{R}_0^s - 1) > 0. \ (a.s).
\end{aligned}$$

As a result, if $\mathbf{R}_0^s > 1$, the infection will remain for an extended period of time. The proof is now complete.

3.3. Ergodicity and stationary distribution

Despite the absence of an endemic equilibrium point in the stochastic framework (2.3), we intend to investigate the existence of an ergodic stationary distribution that potentially shows illness permanence. Furthermore, we present several findings from Has'minskii's approach, see [44].

Suppose there is a homogeneous Markov procedure Θ_d fulfilling the subsequent stochastic DE:

$$d\mathbf{Y}(\xi) = h_1(\mathbf{x}) \mathrm{d}\xi + \sum_{\iota=1}^{\mathbf{n}} \mathcal{G}_{\iota}(\mathbf{Y}) \mathrm{d}\mathcal{B}_{\iota}(\xi). \tag{3.4}$$

The diffusion matrix $A_1(\mathbf{x}) = (a_{\iota\kappa}(\mathbf{x})$ and $a_{\iota\kappa}(\mathbf{x}) = \sum_{\ell=1}^{\mathbf{n}} \mathcal{G}_{\ell}^{(\iota)}(\mathbf{x}) \mathcal{G}_{\ell}^{(\kappa)}(\mathbf{x})$.

Lemma 3.2. *Suppose there is a bounded domain $\mathcal{D} \subset \Theta_d$ having a regular boundary $\mathcal{F}$ such that*

(a) *there is a non-negative number $\mathcal{Q}_1$ such that $\sum_{\iota,\kappa=1}^{d_1} a_{\iota\kappa}(\mathbf{x})\zeta_\iota\zeta_\kappa \geq \mathcal{Q}|\zeta|^2,\ \mathbf{x} \in \mathcal{D}, \zeta \in \mathbf{R}^d$.*

(b) *There exists a positive $\mathbb{C}^2$ mapping $\mathcal{H}$ such that $\mathbb{L}\mathcal{H}$ is negative for each $\mathbf{x} \in \Theta_d \mid \mathcal{D}$, then the Markov technique $\mathbf{Y}(\xi)$ has a one unique ergodic stationary distribution $\pi(.)$ and*

$$\mathbf{P}\Big\{\lim_{\mathbf{T}\mapsto\infty}\frac{1}{\mathbf{T}}\int_0^{\mathbf{T}}\mathcal{F}_1(\mathbf{Y}(\xi))\mathrm{d}\xi = \int_{\Theta_d}\mathcal{F}_1(\mathbf{x})\pi(\mathrm{d}\mathbf{x}) = 1\Big\} \tag{3.5}$$

exists, for $\forall \mathbf{x} \in \Theta_d$, where $\mathcal{F}_1(,)$ is an integrable mapping concerning to measure π.

Theorem 3.3. *For $\mathbf{R}_0^s > 1$ and for initial settings $(\mathbf{s}(0), \mathbf{v}(0), \mathbf{i}(0))$, then the model (2.3) has a unique stationary distribution $\pi(.)$ and it possesses the ergodic behavior.*

Proof. By means of the hypothesis of Theorem 3.1, there is only on global non-negative solution $(\mathbf{s}(\xi), \mathbf{v}(\xi), \mathbf{i}(\xi)) \in \mathbf{R}_+^3$ and for ICs $(\mathbf{s}(0), \mathbf{v}(0), \mathbf{i}(0)) \in \mathbf{R}_+^3$. We simply require to check Suppositions **(a)** and **(b)** of Lemma 3.2 to demonstrate Theorem 3.3. We anticipate obtaining several in order to show **(b)** in the neighbourhood $\mathcal{D} \subset \mathbf{R}_+^3$ and a positive $\mathbb{C}^2$-mapping $\mathcal{H}$ such that $\mathbb{L}\mathcal{H}_s \leq -1$, for every $(\mathbf{s}, \mathbf{v}, \mathbf{i}) \in \mathbf{R}_+^3 \mid \mathcal{D}$. Introducing $\mathbb{C}^2$-mapping $\tilde{\mathcal{H}}$

$$\tilde{\mathcal{H}} = \mathcal{Q}\mathcal{H}_1 - \ln(\mathbf{s}) - \ln(\mathbf{v}) + \frac{1}{1+\varrho}(\mathbf{s}+\mathbf{v}+\mathbf{i})^{\varrho+1}, \tag{3.6}$$

where $\mathcal{H}_1$ is stated in Theorem 3.2, $\mathcal{Q} > 0$ and $\varrho \in (0,1)$ admits

$$\mathcal{F}_1^{u_1} - \mathcal{Q}_1(\omega + \lambda + \frac{\wp_3^2}{2})(\mathbf{R}_0^s - 1) \leq 2 \tag{3.7}$$

and

$$\zeta := \omega - \frac{\varrho}{2}(\wp_1^2 \vee \wp_2^2 \vee \wp_3^2) > 0 \tag{3.8}$$

respectively. Furthermore there is a continuous mapping $\mathcal{F}_1 = -\frac{(1-\mathbf{q})\Xi}{\mathbf{s}} - \frac{\zeta}{2}\mathbf{s}^{\varrho+1} + 2\omega + \vartheta_{\mathfrak{b}} + (1-\phi)\vartheta_\nu + \frac{1}{2}(\wp_1^2 + \wp_2^2)$. We may immediately see that

$$\lim_{\mathbb{k}\mapsto\infty,(\mathbf{s},\mathbf{v},\mathbf{i})\in\mathbf{R}_+^3\mid\mathcal{U}_{\mathbb{k}}}\tilde{\mathcal{H}}(\mathbf{s},\mathbf{v},\mathbf{i}) = \infty, \tag{3.9}$$

where $\mathcal{U}_{\mathbb{k}} = (1/\mathbb{k}, \mathbb{k}) \times (1/\mathbb{k}, \mathbb{k}) \times (1/\mathbb{k}, \mathbb{k})$. Suppose $(\tilde{\mathbf{s}_0}, \tilde{\mathbf{v}_0}, \tilde{\mathbf{i}_0})$ be the lowest point of $\tilde{\mathcal{H}}(\mathbf{s}, \mathbf{v}, \mathbf{i})$. By a positive mapping $\mathcal{H}$, we have

$$\mathcal{H}_s(\mathbf{s}, \mathbf{v}, \mathbf{i}) = \tilde{\mathcal{H}}(\mathbf{s}, \mathbf{v}, \mathbf{i}) - \tilde{\mathcal{H}}(\tilde{\mathbf{s}_0}, \tilde{\mathbf{v}_0}, \tilde{\mathbf{i}_0}). \tag{3.10}$$

Suppose $\mathcal{H}_2 = -\ln \mathbf{s}$, $\mathcal{H}_3 = -\ln \mathbf{v}$ and $\mathcal{H}_4 = \frac{1}{\varrho}(\mathbf{v}+\mathbf{s}+\mathbf{i})^{\varrho+1}$.

Utilizing Itô's technique, we have

$$\mathbb{L}\mathcal{H}_2 \quad = -\frac{(1-\mathbf{q})\Xi}{\mathbf{s}} + (\omega + \frac{\wp_1^2}{2}) + \frac{\vartheta_{\mathfrak{b}}\mathbf{i}}{\mathbf{H}_{\mathfrak{b}} + \mathbf{i}}$$

$$
\begin{aligned}
&\leq (\omega + \vartheta_{\mathfrak{b}} + \frac{\wp_1^2}{2}) - \frac{(1-\mathbf{q})\Xi}{\mathbf{s}},\\
\mathbb{L}\mathcal{H}_3 \quad &= -\frac{\mathbf{q}\Xi}{\mathbf{v}} + (\omega + \frac{\wp_2^2}{2}) + \frac{(1-\phi)\vartheta_\nu \mathbf{i}}{\mathbf{H}_\nu + \mathbf{i}}\\
&\leq (\omega + \vartheta_{\mathfrak{b}} + \frac{\wp_2^2}{2}) + (1-\phi_1)\vartheta_\nu - \frac{\mathbf{q}\Xi}{\mathbf{v}},\\
\mathbb{L}\mathcal{H}_4 \quad &= (\mathbf{s}+\mathbf{v}+\mathbf{i})^{\varrho}\Big\{\Xi - \omega\mathbf{s} - \omega\mathbf{s} - (\omega+\lambda)\Big\} + \frac{\varrho}{2}(\mathbf{s}+\mathbf{v}+\mathbf{i})^{\varrho-1}(\wp_1^2\mathbf{s}^2 + \wp_2^2\mathbf{v}^2 + \wp_3^2\mathbf{i}^2)\\
&\leq \Delta - \frac{\zeta}{2}(\mathbf{s}+\mathbf{v}+\mathbf{i})^{\varrho+1}\\
&\leq \Delta - \frac{\zeta}{2}(\mathbf{s}^{\varrho+1} + \mathbf{v}^{\varrho+1} + \mathbf{i}^{\varrho+1}),
\end{aligned} \tag{3.11}
$$

where $\Delta := \sup_{(\mathbf{s},\mathbf{v},\mathbf{i})\in\mathbf{R}_+^3}\{\Xi(\mathbf{s}+\mathbf{v}+\mathbf{i})^{\varrho} - -\frac{\zeta}{2}(\mathbf{s}+\mathbf{v}+\mathbf{i})^{\varrho+1}\}$. Furthermore, we have

$$
\begin{aligned}
\mathbb{L}\mathcal{H}_s \quad &\leq \mathcal{Q}_1\Big\{-(\omega+\lambda+\frac{\wp_3^2}{2})(\mathbf{R}_0^s - 1) + \Phi_2\mathbf{i}\Big\}\\
&\quad +2\omega + \vartheta_{\mathfrak{b}} + (1-\phi)\vartheta_\nu + \Delta + \frac{1}{2}(\wp_1^2 + \wp_2^1) - \frac{(1-\mathbf{q})\Xi}{\mathbf{s}} - \frac{\mathbf{q}\Xi}{\mathcal{H}} - \frac{\zeta}{2}(\mathbf{s}^{\varrho+1} + \mathbf{v}^{\varrho+1} + \mathbf{i}^{\varrho+1})\\
&:= \mathcal{F}_1(\mathbf{s}) + \mathcal{F}_2(\mathbf{v}) + \mathcal{F}_3(\mathbf{i}),
\end{aligned} \tag{3.12}
$$

where

$$
\begin{aligned}
\mathcal{F}_1(\mathbf{s}) \quad &= -\frac{(1-\mathbf{q})\Xi}{\mathbf{s}} - \frac{\zeta}{2}\mathbf{s}^{\varrho+1} + 2\omega + \vartheta_{\mathfrak{b}} + (1-\phi)\vartheta_\nu + \Delta + \frac{1}{2}(\wp_1^2 + \wp_2^2),\\
\mathcal{F}_2(\mathbf{v}) \quad &= -\frac{\mathbf{q}\Xi}{\mathcal{H}} - \frac{\zeta}{2}\mathbf{v}^{\varrho+1},\\
\mathcal{F}_3(\mathbf{i}) \quad &= -\mathcal{Q}_1(\omega+\lambda+\frac{\wp_3^2}{2})(\mathbf{R}_0^s - 1) + \mathcal{Q}_1\Phi_2\mathbf{i} - \frac{\zeta}{2}\mathbf{i}^{\varrho+1}.
\end{aligned} \tag{3.13}
$$

Therefore, we have
Case I: When $\mathbf{s} \mapsto \infty$ *or* $\mathbf{s} \mapsto 0^+$, then

$$
\mathcal{F}_1(\mathbf{s}) + \mathcal{F}_2(\mathbf{v}) + \mathcal{F}_3(\mathbf{i}) \leq f(\mathbf{s}) + \mathcal{F}_3^{u_1} \mapsto -\infty. \tag{3.14}
$$

Case II: When $\mathbf{v} \mapsto \infty$ *or* $\mathbf{v} \mapsto 0^+$, then

$$
\mathcal{F}_1(\mathbf{s}) + \mathcal{F}_2(\mathbf{v}) + \mathcal{F}_3(\mathbf{i}) \leq \mathcal{F}_2(\mathbf{v}) + \mathcal{F}_1^{u_1} + \mathcal{F}_3^{u_1} \mapsto -\infty. \tag{3.15}
$$

Case III: When $\mathbf{i} \mapsto \infty$, then

$$
\mathcal{F}_1(\mathbf{s}) + \mathcal{F}_2(\mathbf{v}) + \mathcal{F}_3(\mathbf{i}) \leq \mathcal{F}_3(\mathbf{i}) + \mathcal{F}_1^{u_1} + \mathcal{F}_2^{u_1} \mapsto -\infty. \tag{3.16}
$$

This indicates that when $\mathbf{i} \mapsto 0^+$, then

$$
\mathcal{F}_1(\mathbf{s}) + \mathcal{F}_2(\mathbf{v}) + \mathcal{F}_3(\mathbf{i}) \leq \mathcal{F}_3(\mathbf{i}) + \mathcal{F}_1^{u_1} \implies \mathcal{F}_1^{u_1} - \mathcal{Q}_1(\omega+\lambda+\frac{\wp_3^2}{2})(\mathbf{R}_0^s - 1) \leq -2. \tag{3.17}
$$

We define a domain $\mathcal{D} = \Big\{\mathbf{s} \in [\epsilon, 1/\epsilon], \mathbf{v} \in [\epsilon, 1/\epsilon], \mathbf{i} \in [\epsilon, 1/\epsilon]\Big\}$, then

$$\mathbb{L}\mathcal{H}_s(\mathbf{s}, \mathbf{v}, \mathbf{i}) \leq -1, \ \forall (\mathbf{s}, \mathbf{v}, \mathbf{i}) \in \mathbf{R}^3_+ \mid \mathcal{D}. \tag{3.18}$$

Thus, assertion **(b)** satisfies.

However, the diffusion matrix for model (2.3) is defined as

$$\mathcal{A} = \begin{bmatrix} \wp_1^2\mathbf{s}^2 & 0 & 0 \\ 0 & \wp_2^2\mathbf{v}^2 & 0 \\ 0 & 0 & \wp_3^2\mathbf{i}^2 \end{bmatrix}. \tag{3.19}$$

It is simple to demonstrate that there is a $\tilde{c} = \wp_1^2\mathbf{s}^2 \vee \wp_2^2\mathbf{v}^2 \vee \wp_3^2\mathbf{i}^2 > 0$ such that

$$\sum_{\iota,\kappa=1}^{3} a_{\iota\kappa}(\mathbf{s}, \mathbf{v}, \mathbf{i})\zeta_\iota\zeta_\kappa = \wp_1^2\mathbf{s}^2\zeta_1^2 + \wp_2^2\mathbf{v}^2\zeta_2^2 + \wp_3^2\mathbf{s}^2\zeta_3^2 \geq \tilde{c}|\zeta|^2 \tag{3.20}$$

for every $(\mathbf{s}, \mathbf{v}, \mathbf{i}) \in \mathcal{D}$ and $\zeta \in \mathbf{R}^3_+$. Finally, assertion **(a)** satisfies. Therefore, model (2.3) has a unique stationary distribution π and is ergodic.

4. Numerical experiment

We employ the technique of Atangana and Araz described in [28] for the application of the Atangana-Baleanu derivative to validate the numerically piecewise model (2.2) and (2.3). We begin the method as follows:

$$\begin{cases} \frac{\mathrm{d}\chi_\ell(\xi)}{\mathrm{d}\xi} = \Upsilon(\xi, \chi_\ell) = \Upsilon(\xi, \chi_\ell), \ \chi_\ell(0) = \chi_{\ell,0}, \ \ell = 1, 2, ..., \mathbf{n} \ if \ \xi \in [0, \mathbf{T}_1], \\ {}^{ABC}_{\mathbf{T}_1}\mathbf{D}^{\alpha}_{\xi} = \Upsilon(\xi, \chi_\ell), \ \chi_\ell(\mathbf{T}_1) = \chi_{\ell,1}, \ \ell = 1, 2, ..., \mathbf{n} \ if \ \xi \in [\mathbf{T}_1, \mathbf{T}_2], \\ \mathrm{d}\chi_\ell(\xi) = \Upsilon(\xi, \chi_\ell)\mathrm{d}\xi + \wp_\ell\chi_\ell\mathcal{B}_\ell(\xi), \ \chi_\ell(\mathbf{T}_2) = \chi_{\ell,2}, \ \ell = 1, 2, ..., \mathbf{n} \ if \ \xi \in [\mathbf{T}_2, \mathbf{T}]. \end{cases} \tag{4.1}$$

The numerical solution to this problem is provided by

$$\begin{cases} \chi_\ell^{\mathbf{m}_1} = \chi_\ell(0) + \sum\limits_{\kappa=2}^{\mathbf{m}_1} \Big\{\frac{23}{12}\Upsilon(t_\kappa, \chi_\kappa) - \frac{4}{3}\Upsilon(t_{\kappa-1}, \chi_{\kappa-1}) + \frac{5}{12}\Upsilon(t_{\kappa-2}, \chi_{\kappa-2})\Big\}\Delta\xi, \ \ 0 \leq t \leq \mathbf{T}_1, \\ \chi_\ell^{\mathbf{m}_2} = \chi_\ell(\mathbf{T}_1) + \frac{1-\alpha}{ABC(\alpha)}\Upsilon(\xi_{\mathbf{m}_2}, \chi_{\mathbf{m}_2}) + \frac{\alpha(\Delta\xi)^\alpha}{ABC(\alpha)\Gamma(\alpha+1)} \sum\limits_{\mathbf{r}_2=\mathbf{m}_1+3}^{\mathbf{m}_2} \Upsilon(t_{\mathbf{r}_2-2}, \chi_{\kappa_2-2}) \\ \quad \times\Big\{(\mathbf{m}_2 - \mathbf{r}_2 + 1)^\alpha - (\mathbf{m}_2 - \mathbf{r}_2)^\alpha\Big\} + \frac{\alpha(\Delta\xi)^\alpha}{ABC(\alpha)\Gamma(\alpha+2)} \sum\limits_{\kappa_2=\mathbf{m}_1+3}^{\mathbf{m}_2} \Big[\Upsilon(t_{\mathbf{r}_2-1}, \chi_{\mathbf{r}_2-1}) - \Upsilon(t_{\mathbf{r}_2-2}, \chi_{\mathbf{r}_2-2})\Big] \\ \times\Big\{(\mathbf{m}_2 - \mathbf{r}_2 + 1)^\alpha(\mathbf{m}_2 - \mathbf{r}_2 + 3 + 2\alpha) - (\mathbf{m}_2 - \mathbf{r}_2)^\alpha(\mathbf{m}_2 - \mathbf{r}_2 + 3 + 3\alpha)\Big\} \\ \quad + \frac{\alpha(\Delta\xi)^\alpha}{2ABC(\alpha)\Gamma(\alpha+3)} \sum\limits_{\mathbf{r}_2=\mathbf{m}_1+3}^{\mathbf{m}_2} \Big[\Upsilon(t_{\mathbf{r}_2}, \chi_{\mathbf{r}_2}) - 2\Upsilon(t_{\mathbf{r}_2-1}, \chi_{\mathbf{r}_2-1}) + \Upsilon(t_{\mathbf{r}_2-2}, \chi_{\mathbf{r}_2-2})\Big] \\ \quad \times\Big\{(\mathbf{m}_2 - \mathbf{r}_2 + 1)^\alpha(2(\mathbf{m}_2 - \mathbf{r}_2)^2 + (3\alpha + 10)(\mathbf{m}_2 - \mathbf{r}_2) + 2\alpha^2 + p\alpha + 12) \\ \quad -(\mathbf{m}_2 - \mathbf{r}_2)^\alpha(2(\mathbf{m}_2 - \mathbf{r}_2)^2 + (5\alpha + 10)(\mathbf{m}_2 - \mathbf{r}_2) + 6\alpha^2 + 18\alpha + 12)\Big\}, \ \ \mathbf{T}_1 \leq \xi \leq \mathbf{T}_2, \\ \chi_\ell^{\mathbf{m}_3} = \chi_\ell(\mathbf{T}_2) + \sum\limits_{\kappa_3=\mathbf{m}_2+3}^{\mathbf{m}_3} \Big\{\frac{23}{12}\Upsilon(t_{\mathbf{r}_3}, \chi_{\mathbf{r}_3}) - \frac{4}{3}\Upsilon(t_{\mathbf{r}_3-1}, \chi_{\mathbf{r}_3-1}) + \frac{5}{12}\Upsilon(t_{\mathbf{r}_3-2}, \chi_{\mathbf{r}_3-2})\Big\}\Delta\xi \\ \quad + \wp_\ell \sum\limits_{\mathbf{r}_3=\mathbf{m}_2+3}^{\mathbf{m}_3} \chi_\ell^{\mathbf{r}_3}(\mathcal{B}_\ell^{\mathbf{r}_3-1} - \mathcal{B}_\ell^{\mathbf{r}_3}), \ \ \mathbf{T}_2 \leq \xi \leq \mathbf{T}. \end{cases} \tag{4.2}$$

4.1. Results and discussion

Here, we will now apply the piecewise solution scheme presented in [28] to provide a numerical simulation of the developed frameworks (2.1)–2.3 that incorporates the ABC fractional operator. The time is measured in days here. The significance of the parameters used in the simulation can be seen in [10].

Figures 2–4 depicts the dynamical behaviour of HPAI epidemic model with half saturation utilizing the idea of piecewise differential operator in the Atangana-Baleanu sense and stochastic perturbations, respectively. The data analysis conforming to the HPAI models (2.1)–(2.3) outperforms the fractional model results as comparison to the deterministic technique [10] and the technique proposed by [40]. Furthermore, we exhibit chaotic behaviour of the frameworks (2.1)–2.3 involving fractional-order and stochastic disturbances, as seen in Figures 5–8. According to Figures 5–8, reducing interaction between healthy and ignorant persons diminishes the number of diagnosed patients. We conclude that smaller white noise can contribute to illness permanence, whereas larger white noise causes illness extinction. Without a doubt, white noise performs a significant influence in the transmission and prevention of infections. Figures 9 and 10 demonstrates the piecewise view of NPAI models (2.1)–(2.3) utilizing the multiple fractional-orders with environmental intensities $(\wp_1, \wp_2, \wp_3) = (0.01, 0.01, 0.01)$, then $\omega = 0.003699 > \frac{1}{2}(\wp_1^2 \vee \wp_1^2 \vee \wp_1^2) = 0.00015$ and $\mathbf{R}_0^s = 1.1079 > 1$. Theorems 3.2 and 3.3 demonstrate that an ergodic stationary distribution of the stochastic model (2.3) occurs, and the sickness will endure. This is supported by Figures 9 and 10. This emphasis that when fractional-order reduces the disease will die out.

Figures 11–12 explains the behavior of the piecewise framework for distinct parameters settings ω and alongside the recommended stochastic disturbances It is clear that reducing contacts between healthy and HPAI individuals reduces the number of infected individuals.

The findings demonstrate that this novel piecewise differential notion generates improved outcomes for the suggested framework and could potentially be superior for other technological and scientific challenges.

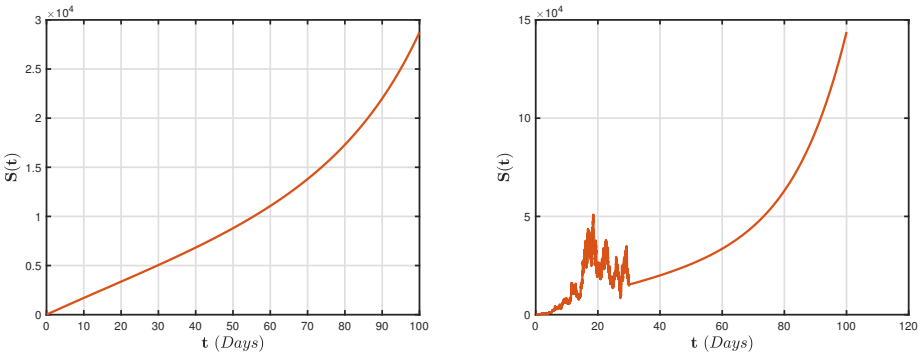

Figure 2. Comparison graphs for the model (2.2) and (2.2) for the susceptible individuals $\mathbf{s}(\xi)$ when $\alpha = 1$ with random densities $\wp_1 = \wp_2 = 0.04$ and $\wp_3 = 0.05$.

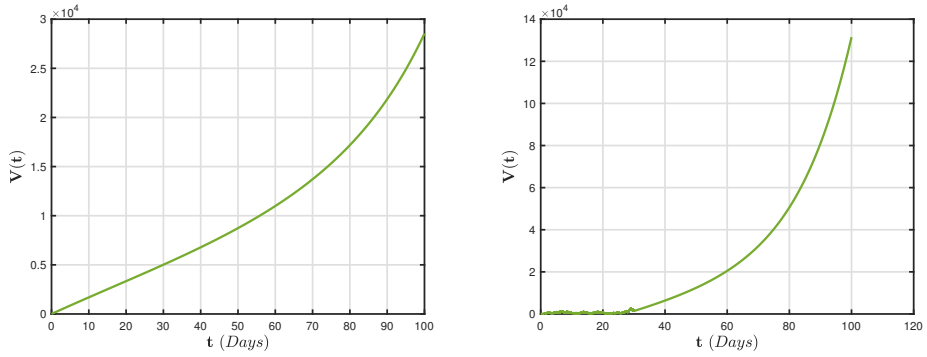

Figure 3. Comparison graphs for the model (2.2) and (2.2) for the vaccinated individuals $\mathbf{v}(\xi)$ when $\alpha = 1$ with random densities $\wp_1 = \wp_2 = 0.04$ and $\wp_3 = 0.05$.

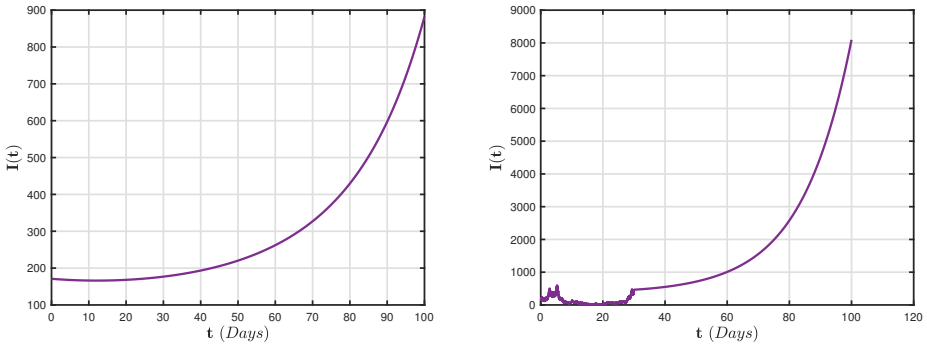

(a) **(b)**

Figure 4. Comparison graphs for the model (2.2) and (2.2) for the infected individuals $\mathbf{i}(\xi)$ when $\alpha = 1$ with random densities $\wp_1 = \wp_2 = 0.04$ and $\wp_3 = 0.05$.

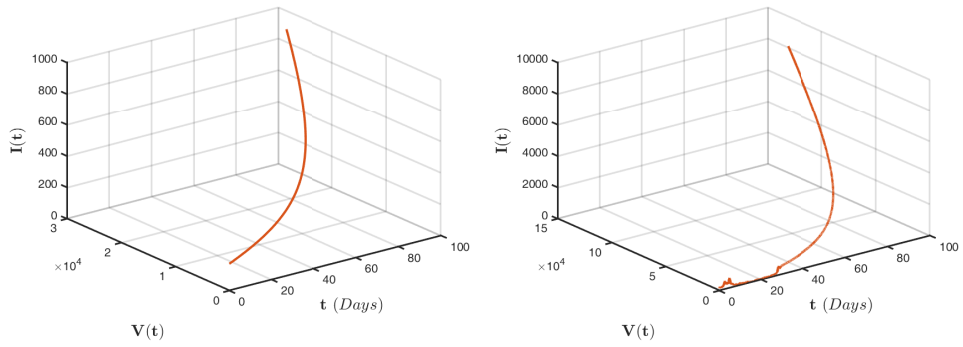

(a) **(b)**

Figure 5. Chaotic behaviour for the model (2.2) and (2.2) for the vaccinated individuals $\mathbf{v}(\xi)$ and infected individuals $\mathbf{i}(\xi)$ when $\alpha = 1$ with random densities $\wp_1 = \wp_2 = 0.04$ and $\wp_3 = 0.05$.

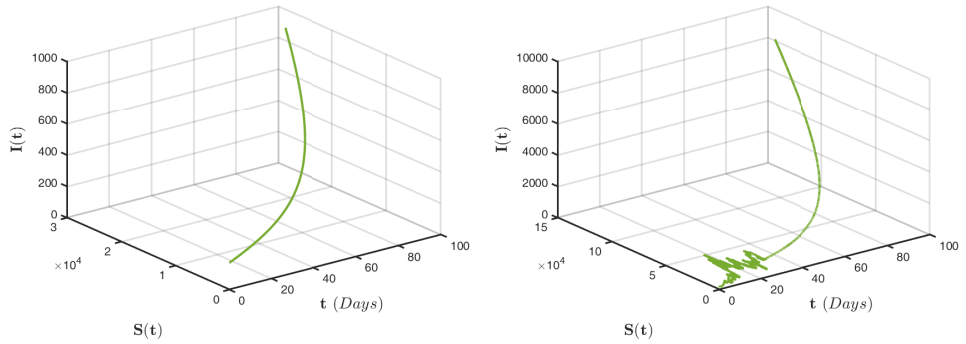

(a) **(b)**

Figure 6. Chaotic behaviour for the model (2.2) and (2.2) for the susceptible individuals $\mathbf{s}(\xi)$ and infected individuals $\mathbf{i}(\xi)$ when $\alpha = 1$ with random densities $\wp_1 = \wp_2 = 0.04$ and $\wp_3 = 0.05$.

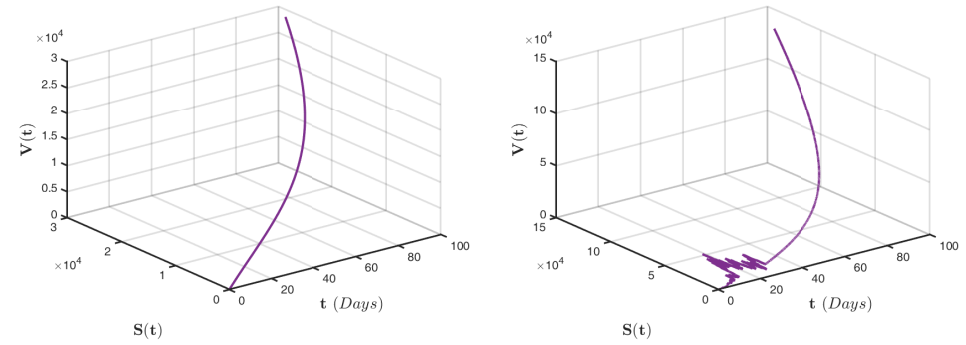

(a) **(b)**

Figure 7. Chaotic behaviour for the model (2.2) and (2.2) for the susceptible individuals $\mathbf{s}(\xi)$ and vaccinated $\mathbf{v}(\xi)$ when $\alpha = 1$ with random densities $\wp_1 = \wp_2 = 0.04$ and $\wp_3 = 0.05$.

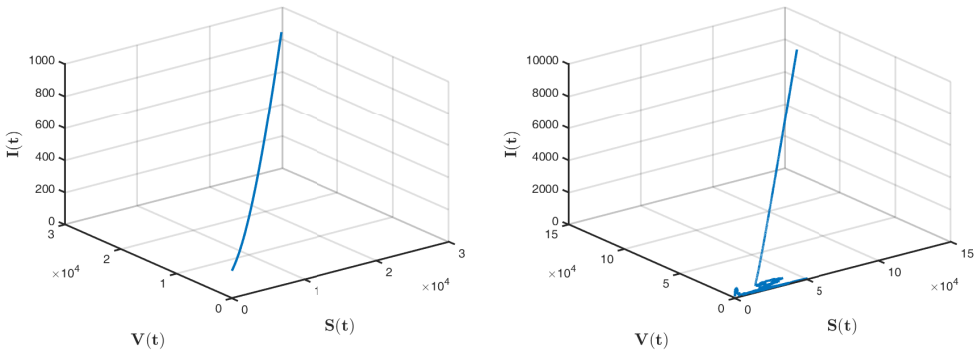

(a) **(b)**

Figure 8. Chaotic behaviour for the model (2.2) and (2.2) for the susceptible individuals $\mathbf{s}(\xi)$, vaccinated $\mathbf{v}(\xi)$ and infected individuals $\mathbf{i}(\xi)$ when $\alpha = 1$ with random densities $\wp_1 = \wp_2 = 0.04$ and $\wp_3 = 0.05$.

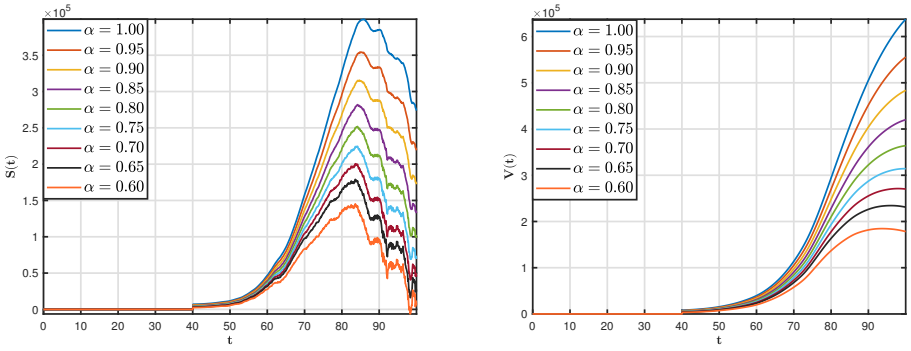

(a) **(b)**

Figure 9. Dynamical behaviour for the model (2.3) for the susceptible individuals $\mathbf{s}(\xi)$ and vaccinated individuals $\mathbf{v}(\xi)$ when random densities $\wp_1 = \wp_2 = \wp_3 = 0.01$ with multiple fractional orders.

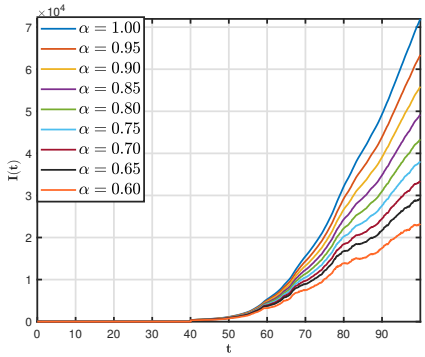

(a)

Figure 10. Dynamical behaviour for the model (2.3) for the infected individuals $\mathbf{i}(\xi)$ when random densities $\wp_1 = \wp_2 = \wp_3 = 0.01$ with multiple fractional order.

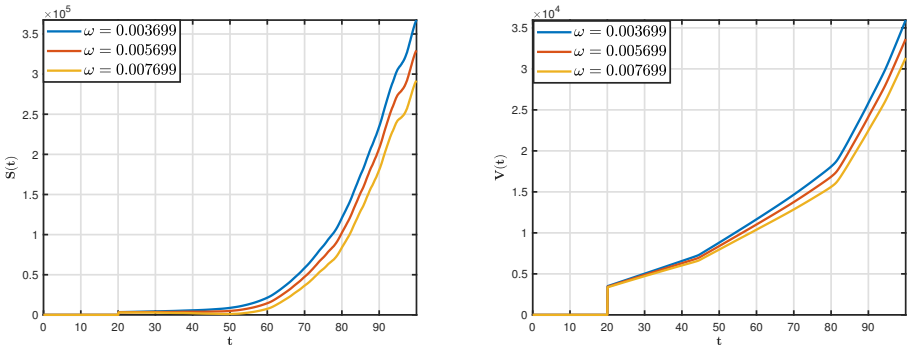

(a) **(b)**

Figure 11. Dynamical behaviour for the model (2.3) for the susceptible individuals $\mathbf{s}(\xi)$ and vaccinated individuals $\mathbf{v}(\xi)$ when random densities $\wp_1 = \wp_2 = \wp_3 = 0.01$, $\alpha = 1$ and varying values of ω.

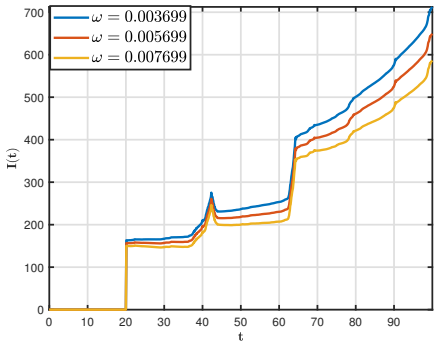

(a)

Figure 12. Dynamical behaviour for the model (2.3) for the infected individuals $\mathbf{i}(\xi)$ when random densities $\wp_1 = \wp_2 = \wp_3 = 0.01$, $\alpha = 1$ with varying values of ω.

5. Conclusions

In this research, we investigate the stochastic HPAI epidemic system having a half saturation transmission level, employing the revolutionary Atangana-Baleanu notion of piecewise fractional differential equation. The framework presented in [10] was expanded to a piecewise structure and its theoretical conclusions were established. Several qualitative aspects of the model are discussed in detail. According to the findings, the approximation utilizing the piecewise approach is superior to that in the systematic review. By employing the notion of Khasminskii and a suitable Lyapunov operator, the existence of a stationary distribution for the model (2.3) was analytically investigated. We investigated the disease's extinction and persistence by proposing the threshold quantity $\mathbb{R}_0^s < 1$. The intensity of environmental noise has been shown to have a significant impact on the persistence of contagious diseases. We anticipated the long-term performance of the structure and demonstrated the consequences of the fractional-order using numerical simulations.

Our research provides several fresh perspectives on HPAI systems consisting of half saturation and may have real-world applications for eradicating epidemics. The main areas will be the emphasis of our future projects: (i) We will conduct a more thorough investigation of the impact of Levy noise on HPAI systems; (ii) In light of recent developments in this domain, we may consider various HPAI neutralizing schemes to simulate stock prices using Monte Carlo simulation; and (iii) Finally, we may broaden this research by using time-delay and trend memory processes by employing the fractional derivative, another useful tool for describing the memory effect.

Conflict of interest

The authors declare that they have no competing interests.

References

1. B. Joob, W. Viroj, H5N6 influenza virus infection, the newest influenza, *Asian Pac. J. Trop. Bio.*, **5** (2015), 434–437. https://doi.org/ 10.1016/j.apjtb.2015.03.001

2. F. Claes, S. Von Dobschuetz, Avian influenza A(H5N6): The latest addition to emerging zoonotic avian influenza threats in east and southeast Asia, *Empres Watch*, **30** (2014).
3. World Health Organization, Weekly epidemiological record Relevpidmiologique hebdomadaire, **92** (2017), 453–476. Available from: `http://www.who.int/wer.`
4. Centers for Disease Control and Prevention, HPAI A H5 virus background and clinical illness. `https://www.cdc.gov/flu/avianflu/hpai/hpai-background-clinical-illness.htm`
5. N. S. Chong, R. J. Smith, Modeling avian influenza using Filippov systems to determine culling of infected birds and quarantine, *Nonlinear Anal. Real*, **24** (2015), 196–218. https://doi.org/10.1016/j.nonrwa.2015.02.007
6. Z. Liu, C. T. Fang, A modeling study of human infections with avian influenza A H7N9 virus in mainland China, *Int. J. Infect. Dis.*, **41** (2015), 73–78. https://doi.org/10.1016/j.ijid.2015.11.003
7. X. Zhang, L. Zou, J. Chen, Y. Fang, J. Huang, J. Zhang, et al., Avian influenza A H7N9 virus has been established in China, *J. Biol. Syst.*, **25** (2017), 605–623. https://doi.org/10.1142/S0218339017400095
8. F. Brauer, C. Castillo-Chavez, *Mathematical models for communicable diseases*, 2012.
9. N. S. Chong, J. M. Tchuenche, R. J. Smith, A mathematical model of avian influenza with half-saturated incidence, *Theory Biosci.*, **133** (2014), 23–38. http://doi.org/10.1007/s12064-013-0183-6
10. S. Liu, S. Ruan, X. Zhang, On avian influenza epidemic models with time delay, *Theory Biosci.*, **134** (2015), 75–82. https://doi.org/10.1007/s12064-015-0212-8
11. S. N. Hajiseyedazizi, M. E. Samei, J. Alzabut, Y. M. Chu, On multi-step methods for singular fractional q-integro-differential equations, *Open Math.*, **19** (2021), 1378–1405. https://doi.org/10.1515/math-2021-0093
12. A. A. Kilbas, O. I. Marichev, S. G. Samko, *Fractional integral and derivatives: Theory and applications*, 1993.
13. K. S. Miller, B. Ross, *An introduction to the fractional calculus and fractional differential equations*, Wiley, 1993.
14. A. A. Kilbas, H. M. Shrivastava, J. J. Trujillo, *Theory and applications of fractional differential equations*, Elsevier, 2006.
15. T. H. Zhao, O. Castillo, H. Jahanshahi, A. Yusuf, M. O. Alassafi, F. E. Alsaadi, et al., A fuzzy based strategy to suppress the novel coronavirus (2019-NCOV) massive outbreak, *Appl. Comput. Math.*, **20** (2021), 160–176.
16. T. H. Zhao, M. I. Khan, Y. M. Chu, Artificial neural networking (ANN) analysis for heat and entropy generation in flow of non-Newtonian fluid between two rotating disks, *Math. Method. Appl. Sci.*, 2021. https://doi.org/10.1002/mma.7310
17. K. Karthikeyan, P. Karthikeyan, H. M. Baskonus, K. Venkatachalam, Y. M. Chu, Almost sectorial operators on Ψ-Hilfer derivative fractional impulsive integro-differential equations, *Math. Method. Appl. Sci.*, **45** (2022), 8045–8059. https://doi.org/10.1002/mma.7954
18. M. Caputo, M. Fabrizio, A new definition of fractional derivative without singular kernel, *Progr. Fract. Differ. Appl.*, **1** (2015), 73–85. https://doi.org/10.12785/pfda/010201

19. A. Atangana, D. Baleanu, New fractional derivatives with non-local and nonsingular kernel: Theory and application to heat transfer model, *Therm. Sci.*, **20** (2016), 763–769. https://doi.org/10.2298/TSCI160111018A

20. Y. M. Chu, U. Nazir, M. Sohail, M. M. Selim, J. R. Lee, Enhancement in thermal energy and solute particles using hybrid nanoparticles by engaging activation energy and chemical reaction over a parabolic surface via finite element approach, *Fractal Fract.*, **5** (2021), 119. https://doi.org/10.3390/fractalfract5030119

21. S. Rashid, S. Sultana, Y. Karaca, A. Khalid, Y. M. Chu, Some further extensions considering discrete proportional fractional operators, *Fractals*, **30** (2022), 2240026. https://doi.org/10.1142/S0218348X22400266

22. S. Rashid, E. I. Abouelmagd, A. Khalid, F. B. Farooq, Y. M. Chu, Some recent developments on dynamical h-discrete fractional type inequalities in the frame of nonsingular and nonlocal kernels, *Fractals*, **30** (2022), 2240110. https://doi.org/10.1142/S0218348X22401107

23. G. Behzad, A. Atangana, A new application of fractional AtanganaBaleanu derivatives: designing ABC-fractional masks in image processing, *Phys. A*, **542** (2020), 123516. https://doi.org/10.1016/j.physa.2019.123516

24. S. Rashid, B. Kanwal, A. G. Ahmad, E. Bonyah, S. K. Elagan, Novel numerical estimates of the pneumonia and meningitis epidemic model via the nonsingular kernel with optimal analysis, *Complexity*, **2022** (2022), 4717663. https://doi.org/10.1155/2022/4717663

25. S. Rashid, A. Khalid, S. Sultana, F. Jarad, K. M. Abualnaja, Y. S. Hamed, Novel numerical investigation of the fractional oncolytic effectiveness model with M1 virus via generalized fractional derivative with optimal criterion, *Results Phys.*, **37** (2022), 105553. https://doi.org/10.1016/j.rinp.2022.105553

26. W. Gao, H. M. Baskonus, L. Shi, New investigation of bats-hosts-reservoir-people coronavirus model and application to 2019-nCoV system, *Adv. Differ. Equ.*, **2020** (2020), 391. https://doi.org/10.1186/s13662-020-02831-6

27. E. F. D. Goufo, Y. Khan, Q. A. Chaudhry, HIV and shifting epicenters for COVID-19, an alert for some countries, *Chaos Soliton. Fract.*, **139** (2020), 110030. https://doi.org/10.1016/j.chaos.2020.110030

28. A. Atangana, S. I. Araz, Modeling third waves of Covid-19 spread with piecewise differential and integral operators: Turkey, Spain and Czechia, *Results Phys.*, **29** (2021), 104694. https://doi.org/10.1016/j.rinp.2021.104694

29. M. A. Khan, H. P. Odinsyah, Fractional model of HIV transmission with awareness effect, *Chaos Soliton. Fract.*, **138** (2020), 109967. https://doi.org/10.1016/j.chaos.2020.109967

30. F. Z. Wang, M. N. Khan, I. Ahmad, H. Ahmad, H. Abu-Zinadah, Y. M. Chu, Numerical solution of traveling waves in chemical kinetics: Time-fractional fishers equations, *Fractals*, **30** (2022), 2240051. https://doi.org/10.1142/S0218348X22400515

31. S. Rashid, E. I. Abouelmagd, S. Sultana, Y. M. Chu, New developments in weighted n-fold type inequalities via discrete generalized h-proportional fractional operators, *Fractals*, **30** (2022), 2240056. https://doi.org/10.1142/S0218348X22400564

32. S. N. Hajiseyedazizi, M. E. Samei, J. Alzabut, Y. M. Chu, On multi-step methods for singular fractional q-integro-differential equations, *Open Math.*, **19** (2021), 1378–1405. https://doi.org/10.1515/math-2021-0093
33. S. A. Iqbal, M. G. Hafez, Y. M. Chu, C. Park, Dynamical analysis of nonautonomous RLC circuit with the absence and presence of Atangana-Baleanu fractional derivative, *J. Appl. Anal. Comput.*, **12** (2022), 770–789. https://doi.org/10.11948/20210324
34. T. H. Zhao, O. Castillo, H. Jahanshahi, A. Yusuf, M. O. Alassafi, F. E. Alsaadi, et al., A fuzzy-based strategy to suppress the novel coronavirus (2019-NCOV) massive outbreak, *Appl. Comput. Math.*, **20** (2021), 160–176.
35. Y. Zhao, E. E. Elattar, M. A. Khan, Fatmawati, M. Asiri, P. Sunthrayuth, The dynamics of the HIV/AIDS infection in the framework of piecewise fractional differential equation, *Results Phys.*, **40** (2022), 105842. https://doi.org/10.1016/j.rinp.2022.105842
36. A. Atangana, S. I. Araz, Modeling and forecasting the spread of COVID-19 with stochastic and deterministic approaches: Africa and Europe, *Adv. Differ. Equ.*, **2021** (2021), 57. https://doi.org/10.1186/s13662-021-03213-2
37. S. Rashid, M. K. Iqbal, A. M. Alshehri, R. Ashraf, F. Jarad, A comprehensive analysis of the stochastic fractalfractional tuberculosis model via Mittag-Leffler kernel and white noise, *Results Phys.*, **39** (2022), 105764. https://doi.org/10.1016/j.rinp.2022.105764
38. M. Al Qurashi, S. Rashid, F. Jarad, A computational study of a stochastic fractal-fractional hepatitis B virus infection incorporating delayed immune reactions via the exponential decay, *Math. Biosci. Eng.*, **19** (2022), 12950–12980. https://doi.org/10.3934/mbe.2022605
39. S. Rashid, R. Ashraf, Q. Asif, F. Jarad, Novel dynamics of a stochastic fractal-fractional immune effector response to viral infection via latently infectious tissues, *Math. Biosci. Eng.*, **19** (2022), 11563–11594. https://doi.org/10.3934/mbe.2022539
40. B. Zhou, X. Zhang, D. Jiang, A Dynamics and density function analysis of a stochastic SVI epidemic model with half saturated incidence rate, *Chaos Soliton. Fract.*, **137** (2020), 109865. https://doi.org/10.1016/j.chaos.2020.109865
41. X. Mao, *Stochastic differential equations and applications*, Horwood Publishing, 1997.
42. X. Mao, G. Marion, E. Renshaw, Environmental Brownian noise suppresses explosions in population dynamics, *Stoch. Proc. Appl.*, **97** (2002), 95–110. https://doi.org/10.1016/S0304-4149(01)00126-0
43. R. Lipster, A strong law of large numbers for local martingales, *Stochastics*, **3** (1980), 217–228. https://doi.org/10.1080/17442508008833146
44. R. Hasminiskii, *Stochastic stability of differential equations*, 1980.